The bipedal Saddle Space: Modelling and validation

The bipedal Saddle Space: Modelling and validation

To cite this article before publication: Carlo Tiseo *et al* 2018 *Bioinspir. Biomim.* in press https://doi.org/10.1088/1748-3190/aae7b0

The Bipedal Saddle Space: Modelling and Validation

C Tiseo[1], K C Veluvolu[2] and W T Ang[1]

[1] Robotic Research Centre, School of Mechanical & Aerospace Engineering, Nanyang Technological University, 50 Nanyang Avenue N3-01a-01, Singapore 639798
[2] School of Electronics Engineering, Kyungpook National University, Daegu, South Korea 702701

E-mail: veluvolu@ee.knu.ac.kr (Kalyana C Veluvolu) ; wtang@ntu.edu.sg (Wei Tech Ang)

Abstract. Better understanding of humans balance control is pivotal for applications such as bipedal robots and medical technologies/therapies targeting human locomotion. Despite the inverted pendulum model being popular to describe the bipedal locomotion, it does not properly capture the step-to-step transition dynamics. The major drawback has been the requirement of both feet on the ground that generates a discontinuity along the intersection of the potential energy surfaces produced by the two legs. To overcome this problem, we propose a generalised inverted pendulum-based model that can describe both single and double support phases. The full characterisation of the system potential energy allows the proposed model to drop the main limitation. This framework also enables to design optimal strategies for the transition between the two feet without the optimisation algorithms. The proposed theory has been validated by comparing the human locomotor strategies output of our planner with real-data from multiple experimental studies. The results show that our model generates trajectories consistent with human variability and performs better compared to existing well-known methods.

Keywords: Human Balance, Bipedal Balance, Inverted Pendulum Model, Extrapolated Centre of Mass, Zero Moment Point, Six Gait Determinant.

1. Introduction

Bipedal stability has been widely studied primarily for medical reasons since the beginning of the last century [1–3]. Over the last few decades, there has been an increasing interest in bipedal locomotion for the development of bipedal robots, assistive devices and rehabilitation technologies for the lower limbs [4–8]. Despite the great effort that has been made by the scientific community, we are just beginning to uncover the mechanisms behind both bipedal balance and locomotion [4, 9, 10]. Among the phenomena that are currently evading our understanding, there is the step-to-step

transition where the traditional inverted pendulum models fail to adequately capture the Centre of Mass (CoM) dynamics [10].

Inverted pendulum-based models are commonly used to describe human locomotion due to their ability to accurately track the CoM trajectory during single support [4,10–12]. On the other hand, they cannot describe the double support phase due to the presence of a discontinuity in the potential energy [13]. To solve this problem existing models employ force-based approach to track the CoM dynamics during double support [10]. As a consequence, bipedal Task-Space (TS) planners rely on numerical planning for handling the foot transition in the double support phase, which is computationally expensive [7, 14].

The Extrapolated Centre of Mass (XCoM), Zero Moment Point (ZMP) and Capture Point (CP) are inverted pendulum-based models that can be used to generate stable foot placements, and can be used to constrain the optimisation process [12, 15, 15–20]. The XCoM uses the limit cycle of inverted pendulum model at a given walking speed. This has become an effective tool to evaluate the limit of stability in human studies [12, 15, 17, 21–24]. The ZMP is a bioinspired model that is mainly employed in bipedal robot controllers [7, 14, 16, 18, 19, 25–32]. It can identify landing positions of the foot based on a given CoM trajectory that needs to be identified *a priori* via optimisation algorithms [7, 14, 16]. The ZMP is calculated through the imposition of a kinematic condition that minimises the angular momentums in the transverse plane [18]. The CP is based on the identification of reachable stability points, which are defined as all the point where dynamics state can be maintained in the orbit of one of the attractor's fixed points. This implies that the system is stable as long as the CoM moves inside the Capture Region (CR) or a new CP can be generated to support the CoM trajectory [16]. The implementation proposed by Pratt and Tedrake defined the margins of the CRs based on a linearised rigid inverted pendulum model [16]. To summarise, the available models are unable to capture the entire dynamics of bipedal systems, and they rely on optimisation algorithms for planning desired CoM trajectories. Therefore, these models are not suited for real-time applications in time-variant environments (i.e., room with moving obstacles) [7, 14, 32].

We propose in this paper a generalised inverted pendulum model based on the analysis of the potential energy surface generated by the two legs. The proposed analytical model is a configuration-dependent Cartesian representation of an inverted pendulum formulated on the hypothesises that humans control the CoM as a simple harmonic oscillator between two maxima of the potential energies generated by the two pendula. Furthermore, the proposed model removes the hypothesis of co-planarity of the pendula required by the inverted pendulum model and integrates existing models (ZMP, the XCoM and CR) in a single framework. Human movements with data obtained from multiple independent studies have been utilised to verify the proposed model [12, 21–23, 33, 34]. The objectives of the paper are:

(i) To prove that human traversal CoM trajectory can be modelled as an oscillator that progresses at a constant velocity with respect to a reference frame aligned with the

anatomical planes, and demonstrate that its potential energy surface can be used to identify a convenient reference frame to describe the system dynamics.

(ii) To verify whether the inability of the inverted pendulum model to track the CoM vertical trajectory is related to the ankle postures.

The model formulation is in Section 2. Subsequently, the validation and the results are described in Section 3, followed by Discussion in Section 4. Section 5 concludes the paper. The derivation of the Saddle point coordinates is included in Appendix A, and Appendix B describes the method to calculate of CoM and extrapolated Centres of Pressure (CoPs) from the reflective markers data.

2. Material and Methods

The model formulation is introduced to the reader at the beginning of this section, while the validation methodology is described later. Table 1 gives a reference about acronyms and definitions used in the model to the reader.

2.1. Model Formulation

The model is based on the formulation of an analytical model of the Potential Field generated by the two legs, modelled as two inverted pendula connected to the same mass via a spherical joint, as shown in Figure 1. Each pendulum is characterised by length (h_{RF} or h_{LF}), the position of its extrapolated CoP (x_{CoPr} or x_{CoPl}), and the shared CoM position (x_{CoM}) which makes the potential energy posture-dependent, as shown in Figures 1 and 2. The extrapolated CoP is defined as the geometrical centre of the area where humans can move the physical centre of pressure within the foot. We have identified the extrapolated CoP using the data reported in [12]. However, this choice is also supported by recent findings where a similar fixed fulcrum of rotation in the foot has been identified from the locomotion kinematics [35]. Lastly, the Base of Support (BoS) is introduced in our model to describe the ability to change the physical centre of pressures that generates a stable range of motion in the vicinity of the extrapolated CoP (Figure 2).

2.1.1. Potential Energy and Saddle Space To determine the shape of the bipedal potential energy, we start the analysis from the hemispheres generated by the two inverted pendula. If the fulcra of the two pendula are sufficiently close, then the two surfaces always intersect along a plane and form a saddle surface. The location of the intersection depends on both the relative position of the fulcra and the lengths of the pendula.

The resultant saddle surface has three fixed points. Two absolute maxima are located above the extrapolated CoPs, and a saddle point located in intersection of the two hemispheres along the segment connecting the two extrapolated CoPs (y_{Saddle} in Figure 1.(a)), that generates a discontinuity. As a consequence, the potential energy

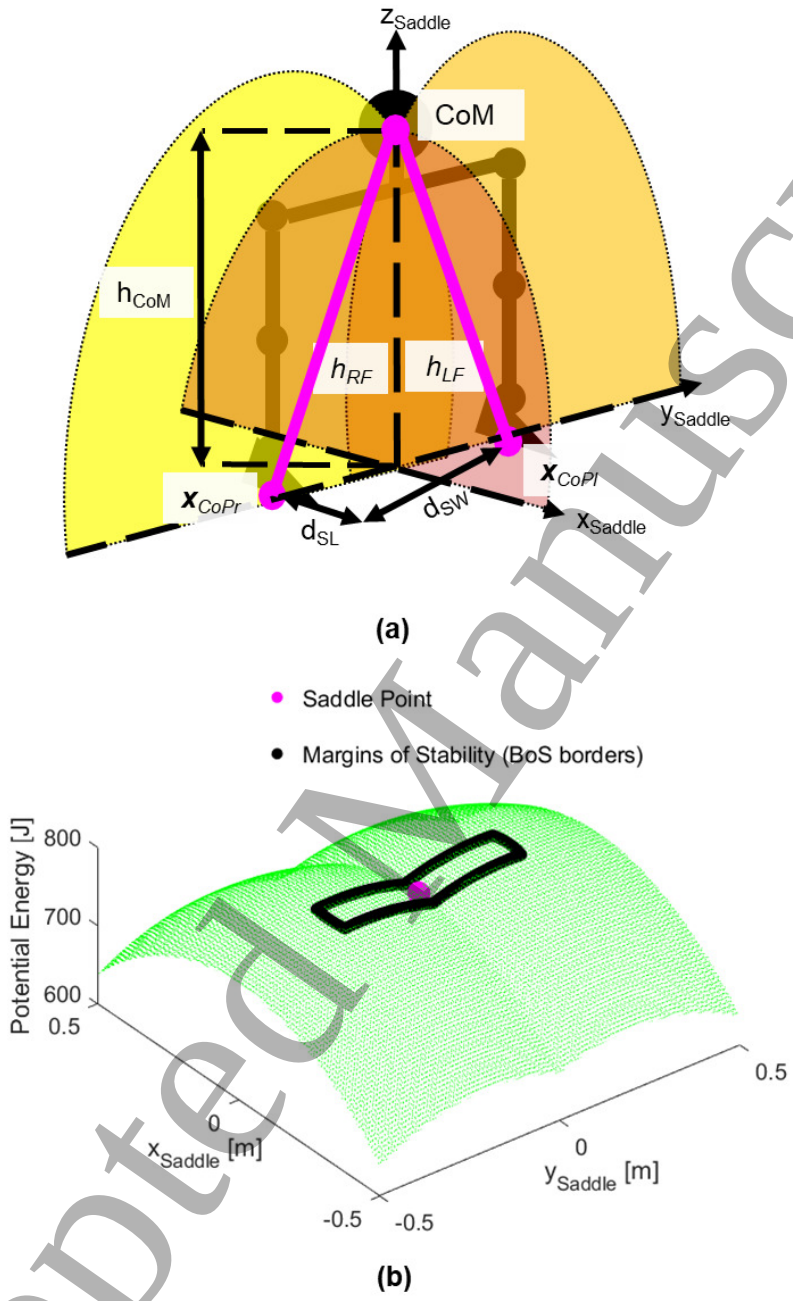

Figure 1. (a) Schematic representation of the saddle principal directions and the definition of the surface reference frame. (b) The potential energy and the Base of Support (BoS) in the SS generated by a system with 80kg CoM, $h_{RF} = 1$ m and $h_{LF} = 1$ m at a distance of 0.2 m. The proposed model produces a map of the potential energy that can be included in the definition of both Margins of Stability (MoS) and the BoS. This allows to express the potential energy as a function of the system kinematics.

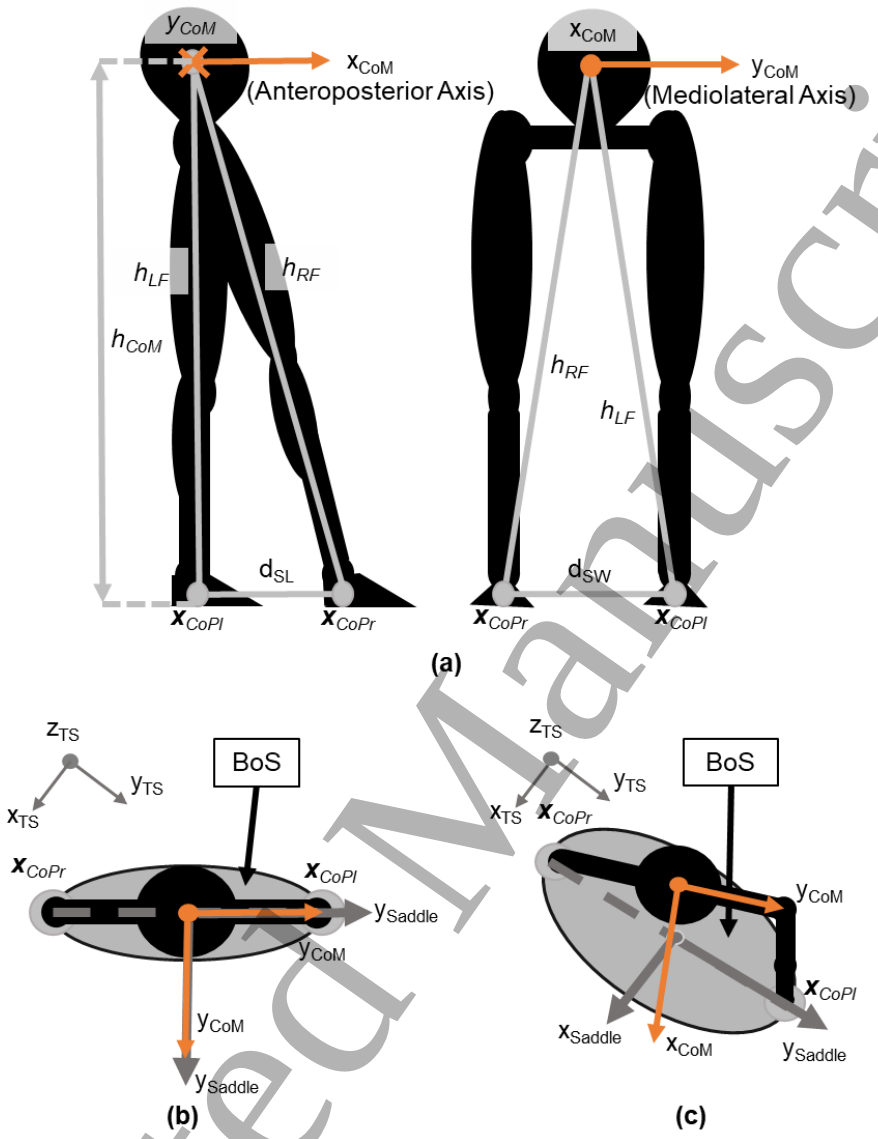

Figure 2. (a) Bipedal systems can be modelled as a mass connected to two pendula of different lengths that provide either double support (both legs sustain the body at the same time) or single support (only one of the pendulum is active). The reference frame chosen in our bipedal model is placed in the centre of mass with the y-axis aligned with the frontal plane (MedioLateral plane ML) lying on the pelvic direction joining the two hip joints. The extrapolated Centre of Pressures (CoPs) are static and placed halfway between the heel and the metatarsus in the middle of the feet. The potential energy of the system is proportional to h_{CoM} that can be then algebraically calculated if d_{SW} (Step Width), d_{SL} (Step Length) and both the pendulum lengths (h_{RF} and h_{LF}) are known. (b) The saddle frame is a posture-dependent frame that is aligned with the anatomical planes when both extrapolated CoPs lay on the frontal plane and, as a consequence, the BoS shape is undistorted in the TS. (c) The BoS is deformed when the body assumes a posture where the extrapolated CoPs do not lie on the frontal plane due to the transformation between the two reference frames.

Table 1. Symbols

SS	Saddle-Space reference frame
(x_{SS}, y_{SS}, z_{SS})	Coordinates expressed in the SS
TS	Task-Space reference frame
(x, y, z)	Coordinates expressed in the TS
CoM	Centre of Mass
CoP	Extrapolated Centre of Pressure
BOS	Base of Support
MoS	Margins of Stability
HS	Heel Strike
TO	Toe Off
v_{des}	Desired walking velocity
A_y	CoM oscillation amplitude in the mediolateral direction
ϕ	Initial phase of the mediolateral oscillation
ω_{Step}	Step frequency or cadence
ω_n	Natural frequency of the inverted pendulum
d_{SL}	Step length
d_{SW}	Step width
U	Potential Energy
$\vec{F}$	Gravitational forces acting on the CoM
M_{CoM}	CoM mass
g	Earth's gravitational acceleration
$\mathbf{x}_{CoPl} = (x_{CoPl}, d_{SW}/2, 0)$	Left extrapolated centre of pressure (CoP) coordinates in the TS
$\mathbf{x}_{CoPr} = (x_{CoPr}, -d_{SW}/2, 0)$	Right extrapolated centre of pressure (CoP) coordinates in the TS
$\mathbf{x}_{CoM} = (x_{CoM}, y_{CoM}, z_{CoM})$	CoM coordinates in the TS
$m_{//}$	The slope of y_{Saddle} in the TS
$m_{\perp}$	The slope of x_{Saddle} in the TS and, consequently, $m_{//} = -1/m_{\perp}$
h_{CoM}	The distance of the CoM from the ground in the TS
h_{RF}	Length of the right pendulum
h_{LF}	Length of the left pendulum
h_{iF0}, $i = R, L$	The base length of the pendulum-based on anthropometrics parameters
h_{body}	Body height
Δh_{iF}, $i = R, L$	Describes the extension of the inverted pendulum due to the foot posture during Heel-Strike
d_h	The distance between the heel and the extrapolated centre of pressure (CoP)
θ_{zFoot}	Describes the angle between the sole of the foot and the ground

cannot be differentiated due to the discontinuity. Therefore, global stability across the border (x_{Saddle} in Figure 1) cannot be evaluated unless the position of the border is known [36].

To eliminate the aforementioned discontinuity, we derived the equations of saddle's two principal directions using euclidean geometry (Appendix A). These equations allow the definition of a posture-dependent reference frame (Saddle Space, SS) that eliminates uncertainty on the position of discontinuity and make the surface differentiable. The SS frame's ordinate (y_{Saddle}) has been defined congruent with the principal direction

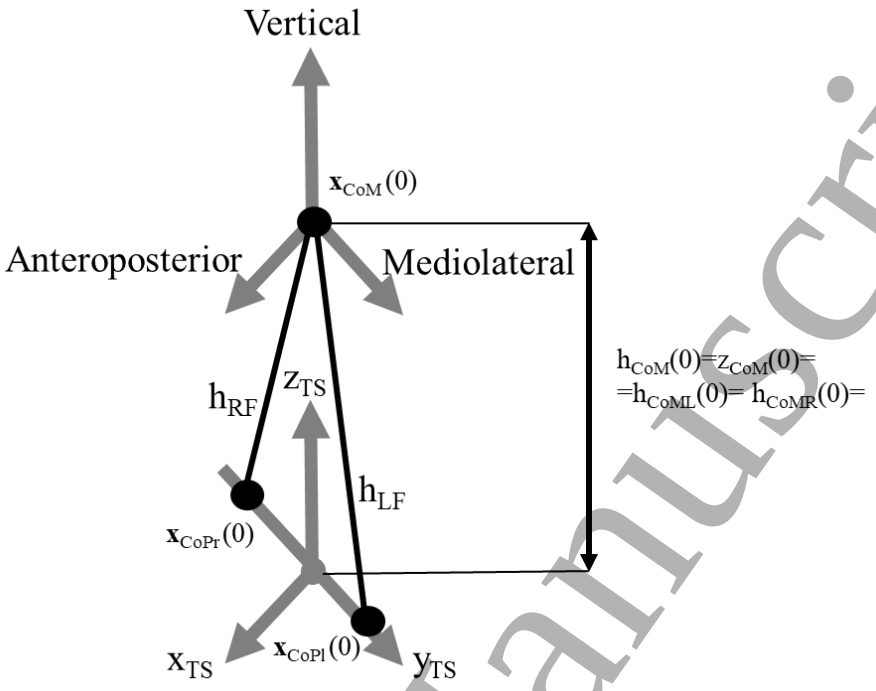

Figure 3. The TS frame employed is aligned with the anatomic axis at t=0, and its transverse plane defines the ground level. Hence, the axis of the TS, SS and CoM frames are aligned for t=0.

between the two maxima of the surface centred in the saddle pointing toward left. As a consequence, the abscissa (x_{Saddle}), is pointing forward and is also centred in the saddle point, as shown in Figures 1 and 2.

The transformation between the TS and the saddle reference frame can now be obtained from the extrapolated CoPs posture as described in Appendix A:

$$\begin{aligned}\begin{bmatrix} x \\ y \end{bmatrix} &= R(\lambda)\vec{x}_{SS} + \vec{x}_{S0} = \\ &= \begin{bmatrix} cos(\lambda) & -sin(\lambda) \\ sin(\lambda) & cos(\lambda) \end{bmatrix} \begin{bmatrix} x_{SS} \\ y_{SS} \end{bmatrix} + \begin{bmatrix} x_{S0} \\ y_{S0} \end{bmatrix}\end{aligned} \tag{1}$$

where $\lambda = \arctan(m_{S_\perp})$ is the angular coefficient of x_{Saddle} in the TS, which is posture-dependent. x_{S0} and y_{S0} are the coordinates of the saddle point that is placed exactly in the centre of the segment connecting the two feet due to the symmetry of human body. Although reconfigurable systems can shift the saddle surface closer to either leg by controlling the lengths of the two legs, we assume that locomotion planning is based on the symmetric configuration.

The identification of the saddle's principal directions in the TS frame allows to track the position of the discontinuity, which enables the formulation of the bipedal system potential energy.

$$U(x,y) = M_{CoM} g z_{CoM} = M_{CoM} g h_{CoM} = \\ = \begin{cases} M_{CoM} g h_{CoML}, & y_{SS-CoM} \geq 0 \\ M_{CoM} g h_{CoMR}, & y_{SS-CoM} < 0 \end{cases} \quad (2)$$

where y_{SS-CoM} is the abscissa of the CoM in the SS, M_{CoM} is the CoM mass, g the gravitational acceleration, h_{RF} is the length of the right pendulum, h_{LF} is the length of the left pendulum, (x_{CoPl}, y_{CoPl}) and (x_{CoPr}, y_{CoPr}) are the coordinates of the left and right extrapolated CoPs respectively. Moreover, h_{CoML} and h_{CoMR} are the height of the CoM with respect to the left extrapolated CoP and the right extrapolated CoP respectively, defined as:

$$h_{CoML} = \sqrt{h_{LF}^2 - (x - x_{CoPl})^2 - (y - y_{CoPl})^2} \\ h_{CoMR} = \sqrt{h_{RF}^2 - (x - x_{CoPr})^2 - (y - y_{CoPr})^2} \quad (3)$$

The main difference between the proposed model and existing models is the elimination of the discontinuity achieved by the definition of the gradient on both sides of the discontinuity along x_{Saddle}. Thus, it facilitates to calculate the gradient of the potential energy [36] as shown below:

$$\vec{F} = -\nabla U(x, y, h_{RF}, h_{LF}) \quad (4)$$

2.1.2. Potential Energy Topology and Bipedal Dynamics The algebraic model of the potential energy provides a tool to analyse the bipedal dynamics without making a priori assumption on the locomotor task and legs kinematic structure. Figure 1.(a) shows that the bipedal system has a stable dynamics along y_{Saddle} between $\mathbf{x}_{CoPl}$ and $\mathbf{x}_{CoPr}$, where the gravitational forces pull the CoM toward the saddle point, and it becomes unstable outside this area. On the other hand, the dynamics of the system is always unstable along x_{Saddle} as the gravity pulls the CoM away from the three fixed points. The sole exception is on the maxima in $x_{SS} = 0$ where $F_{xss} = -\nabla_{xss}(U) = 0$. However, the bipeds may be able to compensate the gravitational forces in a neighbourhood of $x_{SS} = 0$ (i.e., BoS), and the border of such area is the MoS. Nevertheless, they have to generate additional forces to compensate the destabilization along x_{Saddle} which increases the energy expenditure and consequently, reduces the efficiency.

2.1.3. Human Walking Trajectories and Saddle Space The analysis of bipeds dynamics has led to the hypothesis that human walking strategy is planned as a harmonic oscillation (e.g., simple pendulum) centred in the saddle point and constrained to y_{Saddle}, as shown in Figure 4. Such representation requires the harmonic oscillator to complete a full cycle about the saddle point in two steps, which implies a frequency equal to $\omega = \pi\omega_{Step}$.

Therefore, the desired CoM trajectories in the TS can be described as a linear trajectory at constant speed (v_{des}) along x_{TS}, a cosine function with an oscillation

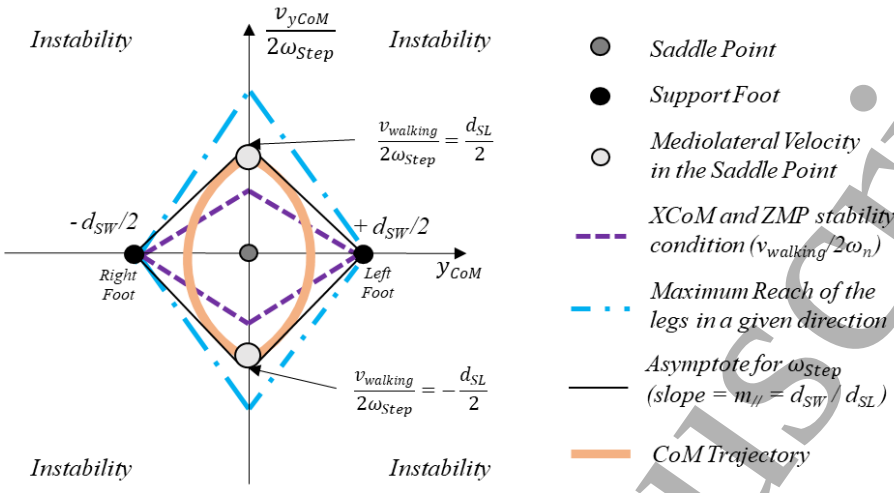

Figure 4. The phase portrait of the CoM dynamics during locomotion when it is represented as an harmonic oscillator centred in the saddle point. The proposed representation can be used to study the system stability, as it enables to visualise if the selected behaviour is in the stable region defined by the legs mechanical properties. The lower limit is the minimum half step length, which is imposed by the natural frequency of the legs and is based on XCoM and ZMP models ($v_{walking}/(2\omega_n)$). The upper limit is the maximum half step length and is determined as the maximum distance that can be reached without jumping.

frequency $\omega = \pi\omega_{Step}$ along y_{TS}, and the vertical trajectory determined from the xy-trajectory using equation (3).

$$\mathbf{x}_{CoM} = \begin{cases} x_{CoM}(t) = v_{des}t \\ y_{CoM}(t) = A_y\cos(\omega t + \phi) = A_y\cos(\pi\omega_{Step}t + \phi) \\ z_{CoM}(t) = \begin{cases} h_{CoML}, & if \quad Left \quad Support \\ h_{CoMR}, & if \quad Right \quad Support \end{cases} \end{cases} \tag{5}$$

where v_{des} is the desired walking speed, A_y is the amplitude of the oscillation, ω_{Step} is the step frequency (cadence), t is the time and ϕ the phase. Furthermore, equation (5) describes the inverted pendulum model in a 3D Cartesian, and if $h_{RF} = h_{LF} = cost$, this model will have the overestimation of the vertical trajectory typical to that of the inverted pendulum model [10,37]. Some models try to address this issue by introducing a variable length of the pendulum to mimic different leg postures during gait [4,10,37]. Subsection 2.1.5 introduces a simplified method for investigating the correlation between the ankle posture and the CoM vertical trajectory during the step-to-step transition.

Nevertheless, the relationships between v_{des}, A_y and ω_{Step} needs to be determined to apply the proposed model. The most intuitive relationship is between the velocity

and the step frequency because the CoM moves forward by 1 step length(d_{SL}) per step; thus, $\omega_{Step} = d_{SL}/v_{des}$.

To identify the relationship between Ay and the gait parameters, the following observations can be obtained based on the dynamics of harmonic oscillators [38] :

(i) The asymptotic behaviour of an oscillator defines the rate of energy exchanged during a period $T = 1/\omega_{Step}$, and its slope is equal to the energy exchanged during a peak-to-peak lateral oscillation of the CoM. This is also used in both ZMP and XCoM to define a stable solution for the step-to-step transition based on the natural frequency of the inverted pendulum [**?**, 7, 12, 15, 17].

(ii) The system potential energy (Figure 1) shows that the optimal trajectory for the step-to-step transition lies on y_{Saddle}. Therefore, the lateral oscillation needs to be tangent to the segment between the two extrapolated CoPs during the transition. This is equivalent to the ZMP model, where the optimal foot placement relies on the minimisation of the angular momentum with the gravitational forces directed towards the landing foot [14, 18] .

(iii) The principle of Covariance implies that all the potential energy accumulated when moving towards a maxima is fully transforms into kinetic energy when the CoM reaches the saddle point.

Based on these three observations the amplitude A_y in equation (5) can be defined as follows:

$$A_y = m_{//step}/(2\pi\omega_{Step}) = d_{SW}/(2\pi\omega_{Step}d_{SL}) \tag{6}$$

where d_{SL} and d_{SW} are the step length and the step width, respectively.

Equation (5) also allows the definition of phase portrait for the system centred in the saddle point, where the abscissa representing the lateral direction and the ordinate describing at the same time the lateral velocity and the anteroposterior placement of the foot, as shown in Figure 4.

2.1.4. Generation of Swinging Foot Anteroposterior Trajectory The formulation of the foot swing trajectory is based on the synchronization observed between anteroposterior trajectory (AP-trajectory) of the foot and the CoM movement in human strategies, and it is equivalent to the compass gait model [4, 39]. To obtain such a condition the CoM trajectory has to be constrained on the segment connecting the two CoPs (i.e., y_{Saddle}), as shown in Figure 5.(a). This locomotor strategy implies that there are no gravitational forces acting perpendicularly to the CoM trajectory that minimises the angular momentum, making it equivalent to the ZMP condition [18].

The following equation describes the AP-trajectory of the feet during swing mention above.

$$\begin{cases} x_{CoPl}(t) = \frac{d_{SW}}{m_{S_{//}}(t)} + x_{CoPr}, & Right \quad Stance \\ \\ x_{CoPr}(t) = \frac{d_{SW}}{m_{S_{//}}(t)} + x_{CoPl}, & Left \quad Stance \end{cases} \tag{7}$$

where $m_{S_{//}}(t) = d_{ML}(t)/d_{AP}(t)$ is the slope of the segment connecting the support foot to the CoM (i.e., y_{Saddle}), which is defined by $d_{ML}(t)$ and $d_{AP}(t)$ that are the instantaneous distances between the two CoPs along the AP and mediolateral (ML) direction, respectively. Lastly, x_{CoPr} and x_{CoPl} are the coordinates of the support foot in the TS. Figure 5.a provides a graphical representation of equation (7).

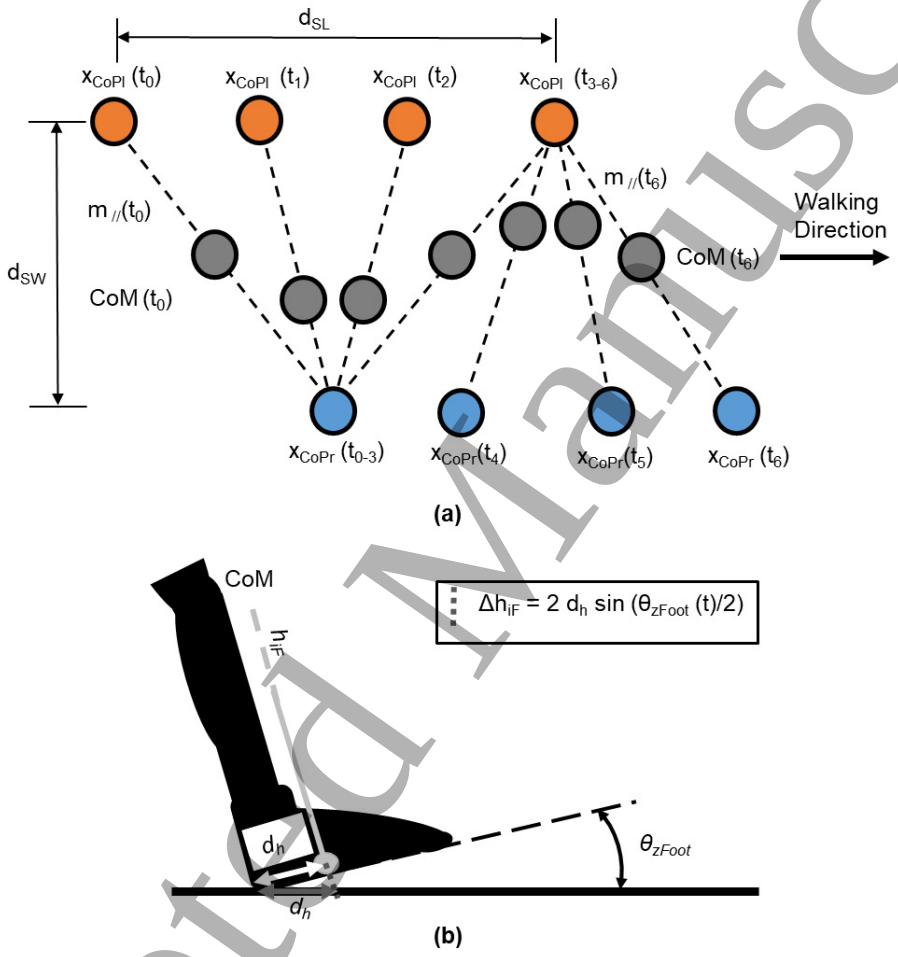

Figure 5. (a) The Swinging Foot AP-Trajectory is generated by imposing the position of the moving foot to be always aligned with the segment between the CoM and the opposite foot as described in equation (7). (b) The heel landing strategy has been modelled not as a rotor-translation of the foot on the ground, but as a reconfiguration in leg length (Δh_{iF}) change which allows to use a static CoP position (extrapolated CoP). The change of length is equal to the chord of a circle with radius d_h.

2.1.5. Heel Strike Model Human legs are fully extended during the Heel Strike (HS) to maximise the efficiency of the movements by maximising the amount support provided by the skeleton [4]. However, even if the length of the pendulum is at its maximum extent there is still a significant misestimation of CoM vertical trajectories [4, 10]. Multiple models have been proposed over the years but they were not able to fully capture the

phenomenon [4].

To address this issue, we have hypothesised that the HS posture and trajectory modifies the pendulum length for the landing foot, thus affecting the CoM trajectory due to the alteration of the saddle trajectory. Defining the pendulum change in length (Δh_{iF}) as represented in Figure 5.b results in the following equation:

$$\begin{aligned} h_{iF} = & \begin{cases} h_{iF0} + \Delta h_{iF}, & \textit{if HS} \\ h_{iF0}, & \textit{otherwise} \end{cases} \\ \textit{where}: & \\ & i = R, L \\ & \Delta h_{iF} = 2 d_h \sin(\theta_{zFoot}(t)/2) \end{aligned} \tag{8}$$

where $d_h = 10$ cm is the distance from the heel of the extrapolated CoP obtained from the data reported by *Hof et al.* [12], $h_{iF0} = 0.57 h_{body}$ is the position of the CoM calculated from the person height (h_{body}) [40], and $\theta_{zFoot}(t)$ is the trajectory of the vertical foot angle during the landing. By updating d_h value to the appropriate contact point, the formulation in equation (8) can be generalised to multiple scenarios, such as walking on a slope or stepping on an object. The correction is included in the model by adding Δh_{iF} to the length of the legs during the heel-strike phase.

2.1.6. Base of Support and Capture Region The CP N-step stability states that a biped locomotion admits a stable solution if it is able to maintain the CoM within the CR for N steps [16]. The CP theory considers two possible strategies for the stability [16]:

(i) Attract the CoM toward a known CP

(ii) Moving a CP to intercept the expected trajectory of the CoM

Consequently, the locomotion can be stabilised as long as the body reconfigures fast enough to enable the CoM trajectory to converge towards a CP [16].

The concept of CP is similar to the dynamic equivalent of the Base of Support (BoS), which is defined as the subset of space where the body is able to counteract the gravitational force [2, 16]. Previous studies have defined multiple BoS shapes in order to describe single and double support postures due to the inability of having a generalised model for the locomotion strategies [11, 12, 41]. In contrary, our BoS formulation is based on the assumption that if the BoS shape in the SS is known (Figure 1), then the BoS shape in TS coordinate can be derived with equation (1). In order to identify the BoS points, the Margins of Stability (MoS) are defined to represent the border between the stable and the unstable subspaces.

The model for BoS presented in this paper is based on the experimental measurements made by Hof *et al.* [12], and its geometrical model has been derived for the single foot base of support as described in [42, 43]. The subjects are in a static posture as in Figure 2.a that allows the SS to be represented undistorted in the TS (equation (1)). Thus it allows us to identify the geometrical shape of the BoS in the SS

that can be described as follows:

$$MoS = \begin{cases} y_{SS}^2 + x_{SS}^2 = CoP_{Ls}^2, & \text{if } y_{SS} \geq 0 \\ & \& \ |x_{SS}| \leq d_h \\ y_{SS}^2 + x_{SS}^2 = CoP_{Rs}^2, & \text{if } y_{SS} \leq 0 \\ & \& \ |x_{SS}| \geq d_h \\ x_{SS} = +d_h, & \text{else if } x_{SS} \geq 0 \\ x_{SS} = -d_h, & \text{else if } x_{SS} \leq 0 \end{cases} \tag{9}$$

$$BoS \leq \quad MoS$$

where $d_h = 10$ cm is the AP range of motion of the extrapolated CoP in the foot [12], and (x_S, y_S) are the coordinates of the SS CoP_{Ls} and CoP_{Rs} are the coordinates of the two extrapolated CoPs in the SS. The MoS obtained with equation (9) are shown in Figure 1.

The identification of model for BoS completes the modelling for double support phase in this paper. In short, the proposed model can be described by the following set of equations:

- Equation (1) defines the transformation between the SS and the TS.
- Equation (5) describes the CoM trajectory in the TS.
- Equation (7) describes the AP-trajectory of the foot during the leg swing.
- Equation (8) describes the increase of the pendulum length generated from the heel stride strategy, which is then used in equation (5).
- Equation (9) describes the shape of the BoS in the SS.

2.2. Validation Method:

The validation is based on the comparison of the model against multiple sets of data to verify the generality of our results. Initially, the model is tested for its ability to reproduce human gait and BoS from postural measurements. Secondly, it is also tested with the motion capture data from the KIT Whole-Body Human Motion DataBase (KITDB) for validation [33]. This allows us to evaluate not only the ability of the system to reproduce a human-like behaviour, but also to identify the presence of abnormalities in the motion.

2.2.1. Validation with Literature Data The ability of the proposed model to reconstruct human-like CoM trajectories (Equations (5) and (7)) is first tested with the data provided by Orendurff *et al.* [34]. The v_{des}, Step Length (d_{SL}) and Step Width (d_{SW})

data are provided as inputs, while the lateral and vertical oscillations are used to compare the proposed model results with the experimental data.

Lastly, the aforementioned postural data during walking have been used for comparing the BoS shape and dimensions predicted by the proposed model with the BoS geometry measurements reported by *McAndrew Young et al.* [22] and *Hak et al.* [23].

2.2.2. Validation with Motion Capture Data The data set used for validation contains 58 trajectories of straight walking movements obtained by the KITDB (MoCap Data). The subjects were 4 males, 2 females age 25 ± 1.7. Their weight and height distributions are 63.3 ± 10.3 kg and 1.79 ± 0.10 m respectively.

The motion capture data allows to validate both the ability of the model to reproduce the CoM trajectories and the effect of the HS on the CoM trajectory. It helps to further investigate the validity of the hypothesis about synchronism that leads to the formulation of equation (7). The CoM trajectory is validated with the motion capture data by comparing the oscillations amplitudes estimated for the vertical and ML directions. Subsequently, the discrepancy between the swinging foot AP trajectory and the one reported in the motion capture data has been evaluated by comparing the angular coefficient of the two curves in the middle of the swinging trajectory, which has been calculated as described in the following equation.

$$m_{swinging} = \frac{x_{foot}(t_{MidSwing}+.04)}{0.8} - \frac{x_{foot}(t_{MidSwing}-.04)}{0.8} \tag{10}$$

where $t_{MidSwing}$ is the time when the swing trajectory is at centre of the take-off and the landing positions.

3. Results

This section reports the validation of our model through the comparison of its output with human locomotor strategies in straight walking. Successful reproduction of human walking behaviour within the range of the variability confirms the validity of the model and the hypothesis.

3.1. Simulations Results

The proposed model estimates the frequencies of oscillation from the velocity and the step length reported by *Orendurff et al.* [34] with a mean error of 2.38 ± 2.06 [steps/minutes], while the behavioural variability across the subjects is minimum at ± 3.4 [steps/minutes]. Similar results are obtained for A_y which is overestimated with an error of 1 ± 1 cm. While ΔZ_{CoM} showed a much higher overestimation error of 3.46 ± 1.35 cm [34].

The results obtained with the KITDB data show an error of 0.7 ± 0.49 cm for the mediolateral CoM trajectory (Figure 6). Instead, the error for the vertical CoM trajectory decreases from 2.18 ± 1.15 cm to 1.43 ± 1.15 cm with the introduction of

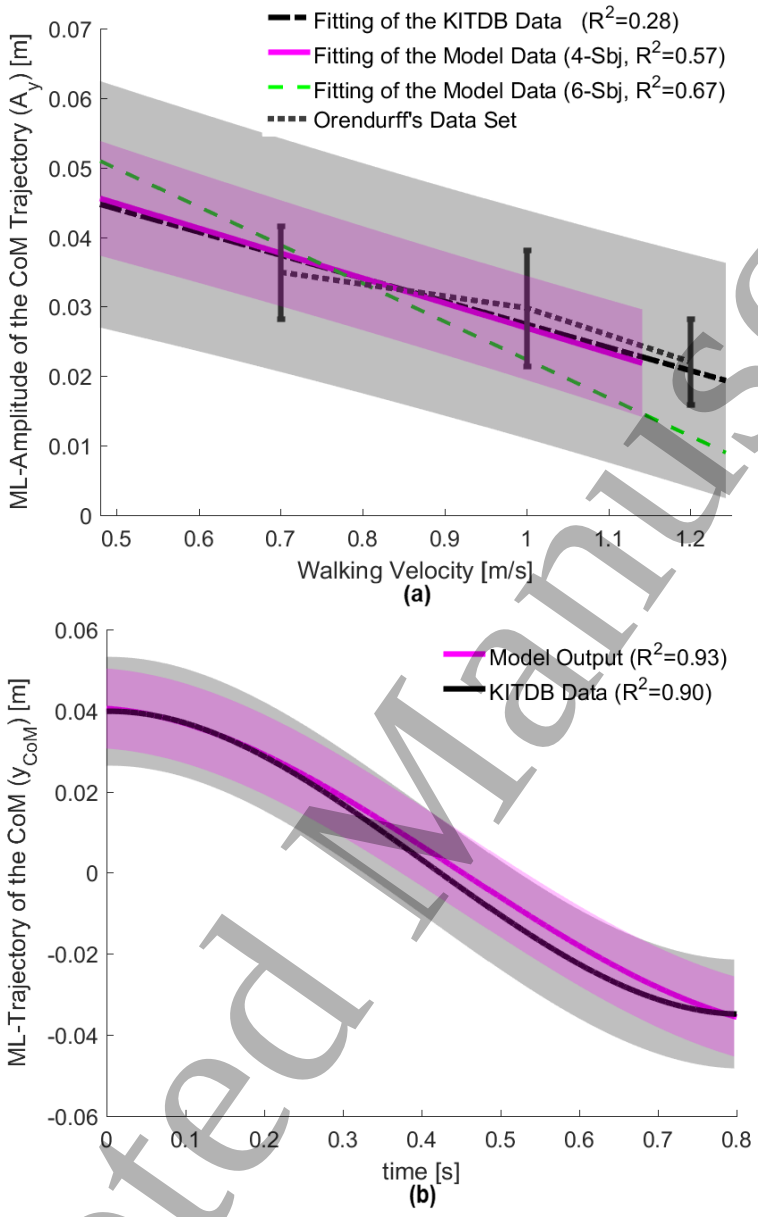

Figure 6. (a) The model performance in estimating A_y shows that the model is able to estimate the motion on the lateral direction with remarkable precision. Although according to *Orendurff et al.* [34] its amplitude variability in human motion is about 1.3 cm, the estimation error of our model is 0.70 ± 0.49 cm. More importantly, it is the ability of the model to detect the abnormal behaviour of subjects 5 and 6 that are both walking with a very small d_{SW}. In fact, if these two subjects are removed from the linear regression, the model output becomes almost collinear with the motion capture data. Lastly, the shaded areas are the 90% prediction bounds of the two fittings. (b) The comparison between the regression curve obtained for the model trajectories is fully enclosed within the 90% prediction bounds of the motion capture data (KITDB Data), which are represented by the two shaded areas.

the HS phase, as shown in Figure 7. Although 45% reduction is obtained with the introduction of the HS model, it is not sufficient to reach accuracy level required for human strategies. This shows that HS is only able to partially justify the discrepancy between our model and the human strategies. The deviation seems related with the effect of the Toe Off (TO) phase, which usually begins about 200 ms before the HS and elevates the trajectory of the CoM [4], as shown in Figure 7.b for one of the analysed trajectories. Instead, Figures 6.b shows how the same CoM trajectory is tracked by our model on the transverse plane.

The results of the swinging foot trajectories model (equation (7)) report estimation error of 8.41 ± 3.75 degrees when compared with the KIT database. The trajectories mainly differ in the saturation behaviour during the phases of TO and HS as shown in Figure 8.

The Figure 9 shows the BoS shape and dimensions of walking postures consistent with the previous observations [12, 21–23, 41, 44]. It has been reported by *McAndrew Young et al.* [22] that the AP dimension is between 0.8m to 1 m, while the ML ranges are between 0.1 to 0.15 m. Further, the shape proposed by *McAndrew Young et al.* [22] is a less detailed rectangular shape with a qualitative classification of 4 sub-quadrant, while equation (9) produces a diagonal shape consistent with the majority of the data for the BoS shape [12,21,41,44]. Furthermore, *Hak et al.* [23] reported how humans adjust their frequency and step length to maintain their progression velocity without compromising their stability, but increasing their metabolic expenditure. This is congruent with the behaviour of the BoS shape reported in Figure 9 where the BOS ML dimension increases with the shortening of the steps. This proves how the proposed model can describe the BoS shape without the necessity of using different models for the single and double support phases.

4. Discussion

The main purpose of this study is to identify a generalised balance model that can describe both single and double support stances. The results obtained show that this model can derive the CoM trajectory by measuring the motion of the feet and *vice versa*. Particularly, the model can generate a swinging trajectory of the foot similar to the ZMP model as shown in Figure 6. Furthermore, the A_y formulation (equation (5)) converges to the XCoM model trajectory when the oscillation frequency approaches the natural frequency [12, 15, 17, 28]. This implies that the proposed formulation provides the placement of the extrapolated CoP within the stability limit identified by the XCoM model [12].

4.1. The Importance of step-to-step transition phase in Balance

The HS model can partially correct the error made in the vertical estimation of the CoM trajectory that underlies the presence of other factors influencing the motion. Figure

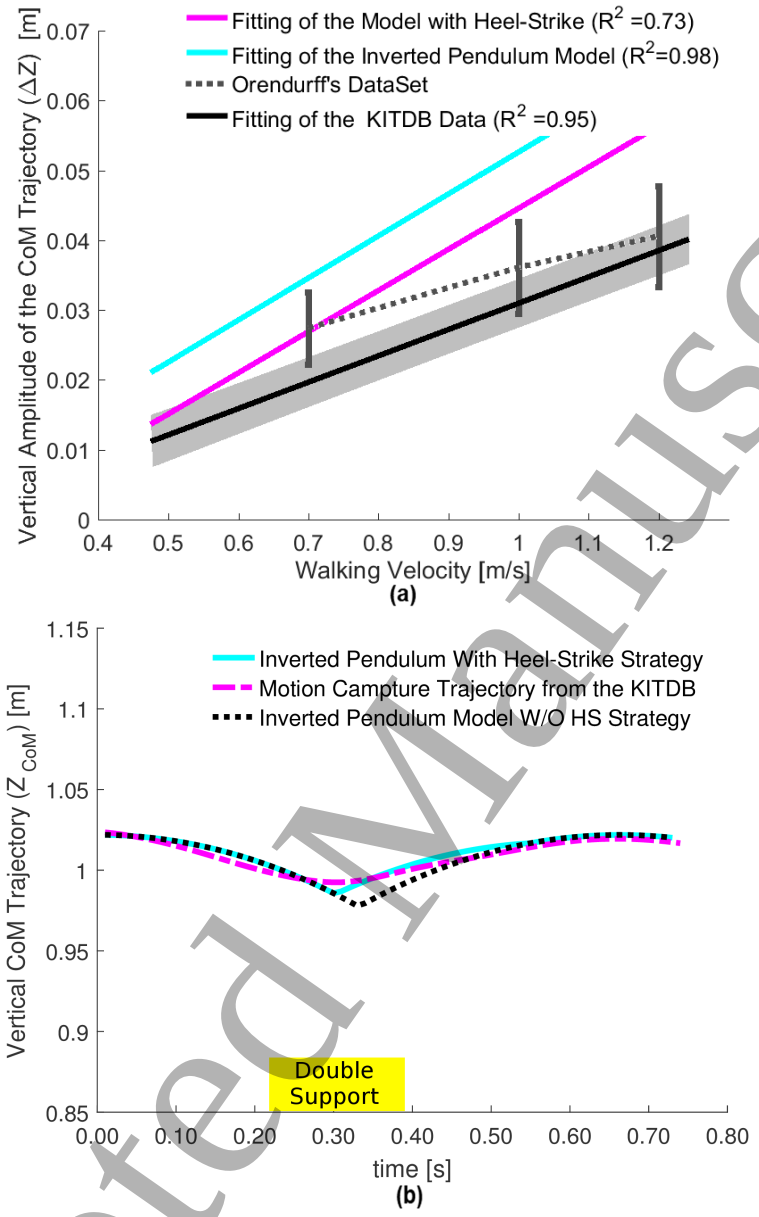

Figure 7. (a) The estimation of the CoM height variation during gait provides further support to the performances of this model, and it also underlines the fact that the HS strategy is not the sole issue that influences the CoM vertical trajectory. Despite the approximations, the estimation error across the subjects is consistent with the variability observed in human subjects reported by *Orendurff et al.* [34]. The error obtained with the HS model is 1.43 ± 1.15 cm whereas the error obtained without the HS model is 2.18 ± 1.15 cm. The shaded area represents the 90% prediction bounds of the fitting for the vertical movement data. (b) Comparing the measured CoM trajectory with the one obtained by the model at a walking speed of 0.81 m/s, it is possible to appreciate how even a simple model of the HS allows for a more precise approximation of the measured data. The duration double support phase in the human trajectory is highlighted in yellow, and it rappresents the 27% of the step duration.

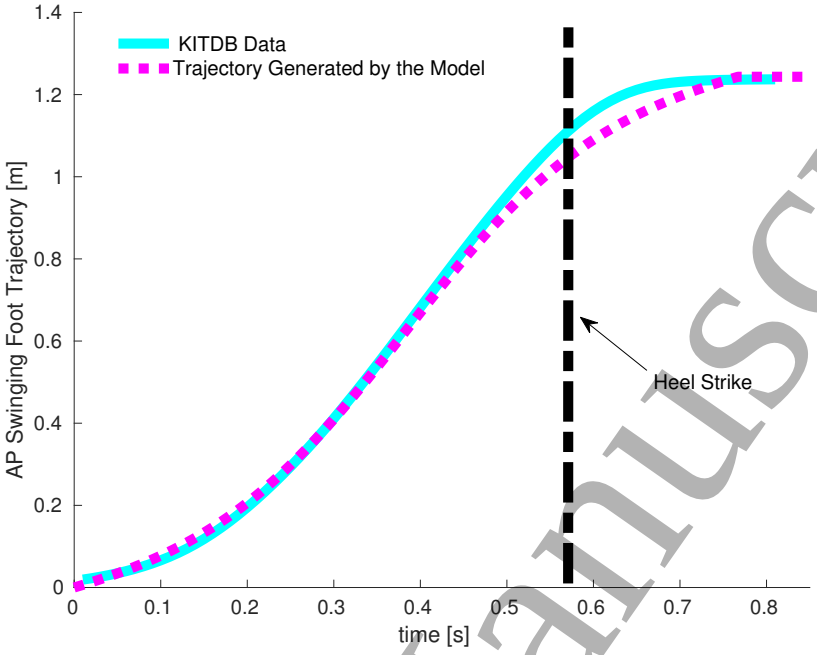

Figure 8. The hypotheses of synchronism between the saddle and the CoM allows to generate trajectory in the AP direction which is consistent with human movements. The only exception is for the terminal part of the trajectory during HS where the motion of the saddle is altered by the step-to-step transition strategy, as shown in this figure for a speed of 0.81 m/s. Moreover, the trajectory generated with our method exhibits a similar behaviour compared to the ZMP model presented by *Kima et al.* [28].

7.b shows the importance of having a precise assessment of the step-to-step transition because small changes in these strategies generate significant variations in the potential energy. This implies that the vertical movements of the CoM are actively controlled by the system to provide or absorb excess energy needed to implement a more efficient balance control. Moreover, there is evidence that the ankle plays the central role in the implementation of such strategies. Previous studies underlined the importance of the ankle strategies for both the balance control and the gait efficiency, which lead to the development of a broad spectrum of devices targeting the ankle for rehabilitation and assistive applications [5, 8, 11, 45–48].

4.2. Implication of having a unique BoS

The BoS and MoS (equation (9)) can be expressed in TS coordinates with equation (1) allowing to reproduce results equivalent to the results reported by both *McAndrew Young et al.* [22] and *Hak et al.* [23]. This demonstrates the potential of this model to supervise balance required by the application and also to gain a better understanding of how the nervous system can control the body equilibrium. However, the BoS model requires further refinement, for example, the introduction of the foot orientation in the

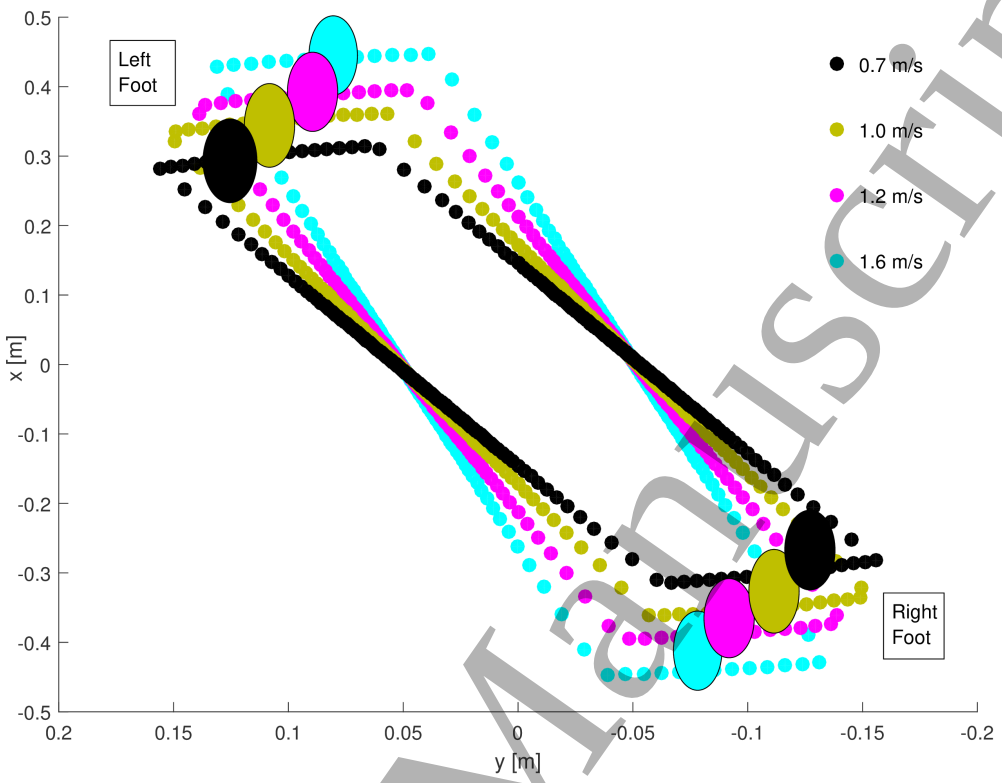

Figure 9. The BoS is heavily dependent on the extrapolated CoPs' positions. The postures assumed while walking at 0.7, 1.0, 1.2 and 1.6 m/s as reported by *Orendurff et al.* [34] are compared to analyse how the stepping strategies modify the BoS with the increase in speed and, diverts the system stability towards the motion direction and, thus limits the lateral stability. Such behaviours are consistent with previous observations, which report humans using shorter steps at a higher frequency in order to obtain greater lateral stability without reducing the walking speed [23,39]. Lastly, the MoS produced by our model is congruent with the experimental results in *McAndrew Young et al.* [22].

transverse plane will allow to better account for the anisotropic behaviour of the legs.

4.3. Computational performances

The simple model formulation allows having an execution time of 0.82 ms per MoS and 2.25 ms per step trajectory. The simulations were conducted using Matlab running on a laptop with Windows 10. The processor is Intel i7-4710HQ, the RAM is 16 GB DDR3. This enables not only the possibility of implementing a real-time balance supervision system needed for the Mobile Robotic Assistive Balance Trainer control, but it may also lead to a real-time balance assessment of the patient.

4.4. Future Work

To complete the development of the balance model, we will focus on the identification of the stability conditions, the improvement of the BoS model and the study of the relationships between the different gait parameters. Once the stability conditions are identified, the model also has the potential for being used in bipedal robot high-level controllers, thus providing a cost-effective alternative to trajectory planning and supervision.

5. Conclusion

The proposed balance model represents the human walking strategies within the range of human variability. It does not contradict other gait and balance models but instead, includes them in a single framework. The proposed model is a computationally inexpensive tool that has the potential to improve our understanding of bipedal locomotion in unstructured environments. Thus, it represents a first step in the development of a balance model that can evaluate bipedal stability from the body kinematics without measuring the ground reaction forces.

Furthermore, we have been able to prove that human planning strategy considers their legs as coupled reconfigurable mechanical oscillators. Thus it explains why the legs behave like non-linear oscillators [46], which underlines the potential of this approach not only in describing human behaviours but also for studying human balance motor control. Lastly, the proposed approach can also contribute in humanoid robotics, being an extension of existing models that are commonly used in bipedal robots (i.e. ZMP, CP and CR).

Acknowledgments

This research was supported by the A*STAR-NHG-NTU Rehabilitation Research Grant: "Mobile Robotic Assistive Balance Trainer" (RRG/16018). This work has been extracted from the PhD Thesis of Carlo Tiseo [42].

References

[1] J B Saunders, V T Inman, and H D Eberhart. The major determinants in normal and pathological gait. *The Journal of bone and joint surgery. American volume*, 35-A(3):543–58, Jul 1953.

[2] A.S. Pollock, B.R. Durward, P.J. Rowe, and J.P. Paul. What is balance? *Clinical Rehabilitation*, 14(4):402–406, Aug 2000.

[3] F E Huxham, P a Goldie, and a E Patla. Theoretical considerations in balance assessment. *The Australian journal of physiotherapy*, 47(2):89–100, Jan 2001.

[4] Diego Torricelli, Jose Gonzalez, Maarten Weckx, René Jiménez-Fabián, Bram Vanderborght, Massimo Sartori, Strahinja Dosen, Dario Farina, Dirk Lefeber, and Jose L Pons. Human-like compliant locomotion: state of the art of robotic implementations. *Bioinspiration & Biomimetics*, 11(5):051002, Aug 2016.

[5] Serena Maggioni, Alejandro Melendez-Calderon, Edwin van Asseldonk, Verena Klamroth-Marganska, Lars Lünenburger, Robert Riener, and Herman van der Kooij. Robot-aided assessment of lower extremity functions: a review. *Journal of NeuroEngineering and Rehabilitation*, 13(1):72, Dec 2016.

[6] Tad McGeer. Passive Dynamic Walking. *The International Journal of Robotics Research*, 9(2):62–82, Apr 1990.

[7] Justin Carpentier, Steve Tonneau, Maximilien Naveau, Olivier Stasse, and Nicolas Mansard. A versatile and efficient pattern generator for generalized legged locomotion. In *2016 IEEE International Conference on Robotics and Automation (ICRA)*, pages 3555–3561. IEEE, May 2016.

[8] Iñaki Díaz, Jorge Juan Gil, and Emilio Sánchez. Lower-Limb Robotic Rehabilitation: Literature Review and Challenges. *Journal of Robotics*, 2011(i):1–11, 2011.

[9] B E Maki and W E McIlroy. Cognitive demands and cortical control of human balance-recovery reactions. *Journal of Neural Transmission*, 114(10):1279–1296, Oct 2007.

[10] Arthur D Kuo. The six determinants of gait and the inverted pendulum analogy: A dynamic walking perspective. *Human Movement Science*, 26(4):617–656, Aug 2007.

[11] DA Winter. Human balance and posture control during standing and walking. *Gait & Posture*, 3(4):193–214, Dec 1995.

[12] A.L. Hof, M.G.J. Gazendam, and W.E. Sinke. The condition for dynamic stability. *Journal of Biomechanics*, 38(1):1–8, Jan 2005.

[13] Ippei Obayashi, Shinya Aoi, Kazuo Tsuchiya, and Hiroshi Kokubu. Formation mechanism of a basin of attraction for passive dynamic walking induced by intrinsic hyperbolicity. *Proceedings of the Royal Society A: Mathematical, Physical and Engineering Science*, 472(2190):20160028, Jun 2016.

[14] Stephane Caron, Quang-Cuong Pham, and Yoshihiko Nakamura. ZMP Support Areas for Multicontact Mobility Under Frictional Constraints. *IEEE Transactions on Robotics*, pages 1–14, 2016.

[15] At L Hof. The extrapolated center of mass' concept suggests a simple control of balance in walking. *Human Movement Science*, 27(1):112–125, Feb 2008.

[16] J.E. Pratt and R. Tedrake. Velocity-Based Stability Margins for Fast Bipedal Walking. In *Fast Motions in Biomechanics and Robotics*, pages 299–324. Springer Berlin Heidelberg, Berlin, Heidelberg, 2006.

[17] At L Hof, Renske M van Bockel, Tanneke Schoppen, and Klaas Postema. Control of lateral balance in walking. *Gait & Posture*, 25(2):250–258, Feb 2007.

[18] Miomir Vukobtatović, Hugh M. Herr, Branislav Borovac, Mirko Raković, Marko Popovic, Andreas Hofmann, MiloŠ Jovanović, and Veljko Potkonjak. Biological Principles of Control Selection for a Humanoid Robot's Dynamic Balance Preservation. *International Journal of Humanoid Robotics*, 05(04):639–678, Dec 2008.

[19] Andreas Hofmann, Marko Popovic, and Hugh Herr. Exploiting angular momentum to enhance bipedal center-of-mass control. In *2009 IEEE International Conference on Robotics and Automation*, pages 4423–4429. IEEE, May 2009.

[20] M. Popovic, A. Hofmann, and H. Herr. Angular momentum regulation during human walking: biomechanics and control. In *IEEE International Conference on Robotics and Automation, 2004. Proceedings. ICRA '04. 2004*, volume 3, pages 2405–2411 Vol.3. IEEE, 2004.

[21] Vipul Lugade, Victor Lin, and Li-shan Chou. Center of mass and base of support interaction during gait. *Gait & Posture*, 33(3):406–411, Mar 2011.

[22] Patricia M McAndrew Young and Jonathan B Dingwell. Voluntary changes in step width and step length during human walking affect dynamic margins of stability. *Gait & Posture*, 36(2):219–224, Jun 2012.

[23] Laura Hak, Han Houdijk, Peter J. Beek, and Jaap H. van Dieën. Steps to Take to Enhance Gait Stability: The Effect of Stride Frequency, Stride Length, and Walking Speed on Local Dynamic

Stability and Margins of Stability. *PLoS ONE*, 8(12):e82842, Dec 2013.

[24] M Vlutters, E. H. F. van Asseldonk, and H. van der Kooij. Center of mass velocity-based predictions in balance recovery following pelvis perturbations during human walking. *The Journal of Experimental Biology*, 219(10):1514–1523, May 2016.

[25] Stefan Czarnetzki, Sören Kerner, and Oliver Urbann. Observer-based dynamic walking control for biped robots. *Robotics and Autonomous Systems*, 57(8):839–845, Jul 2009.

[26] Shuhei Shimmyo, Tomoya Sato, and Kouhei Ohnishi. Biped Walking Pattern Generation by Using Preview Control Based on Three-Mass Model. *IEEE Transactions on Industrial Electronics*, 60(11):5137–5147, Nov 2013.

[27] Sungho Jo and Steve G Massaquoi. A model of cerebrocerebello-spinomuscular interaction in the sagittal control of human walking. *Biological Cybernetics*, 96(3):279–307, Mar 2007.

[28] Jung-Hoon Kima, Jong Hyun Choib, and Baek-Kyu Choc. Walking Pattern Generation for a Biped Walking Robot Using Convolution Sum. *Advanced Robotics*, 25(9-10):1115–1137, Jan 2011.

[29] Josep M. Font-Llagunes and József Kövecses. Dynamics and energetics of a class of bipedal walking systems. *Mechanism and Machine Theory*, 44(11):1999–2019, Nov 2009.

[30] Xiang Luo and Wenlong Xu. Planning and Control for Passive Dynamics Based Walking of 3D Biped Robots. *Journal of Bionic Engineering*, 9(2):143–155, Jun 2012.

[31] Kojiro Matsushita, Hiroshi Yokoi, and Tamio Arai. Pseudo-passive dynamic walkers designed by coupled evolution of the controller and morphology. *Robotics and Autonomous Systems*, 54(8):674–685, Aug 2006.

[32] M. Popovic, A. Hofmann, and H. Herr. Zero spin angular momentum control: definition and applicability. In *4th IEEE/RAS International Conference on Humanoid Robots, 2004.*, volume 1, pages 478–493. IEEE, 2004.

[33] Christian Mandery, Omer Terlemez, Martin Do, Nikolaus Vahrenkamp, and Tamim Asfour. The KIT whole-body human motion database. In *2015 International Conference on Advanced Robotics (ICAR)*, volume 611909, pages 329–336. IEEE, Jul 2015.

[34] Michael S Orendurff, Ava D Segal, Glenn K Klute, Jocelyn S Berge, Eric S Rohr, and Nancy J Kadel. The effect of walking speed on center of mass displacement. *Journal of rehabilitation research and development*, 41(6A):829–34, 2004.

[35] Justin Carpentier, Mehdi Benallegue, and Jean-Paul Laumond. On the centre of mass motion in human walking. *International Journal of Automation and Computing*, 2017.

[36] Peter Gilkey, JeongHyeong Park, and Ramon Vazquez-Lorenzo. *Aspects of Differential Geometry I*. Morgan & Claypool, 2015.

[37] W. Zijlstra and A.L. Hof. Displacement of the pelvis during human walking: experimental data and model predictions. *Gait & Posture*, 6(3):249–262, Dec 1997.

[38] Steven H Strogatz. *Nonlinear dynamics and chaos: with applications to physics, biology, chemistry, and engineering*. Hachette UK, 2014.

[39] Carlo Tiseo and Wei Tech Ang. The Balance: An energy management task. In *2016 6th IEEE International Conference on Biomedical Robotics and Biomechatronics (BioRob)*, pages 723–728. IEEE, Jun 2016.

[40] Mikko Virmavirta and Juha Isolehto. Determining the location of the body s center of mass for different groups of physically active people. *Journal of Biomechanics*, 47(8):1909–1913, Jun 2014.

[41] Y C Pai and James Patton. Center of mass velocity-position predictions for balance control. *Journal of biomechanics*, 30(4):347–54, Apr 1997.

[42] Carlo Tiseo. *Modelling of bipedal locomotion for the development of a compliant pelvic interface between human and a balance assistant robot*. PhD thesis, Nanyang Technological University, 2018.

[43] Carlo Tiseo, Kalyana C Veluvolu, and Wei Tech Ang. Evidence of a Clock Determining Human Locomotion. In *2018 40th Annual International Conference of the IEEE Engineering*

in Medicine and Biology Society, EMBC 2018, 2018.

[44] Y C Pai and Kamran Iqbal. Simulated movement termination for balance recovery: can movement strategies be sought to maintain stability in the presence of slipping or forced sliding? *Journal of biomechanics*, 32(8):779–86, Aug 1999.

[45] Andrew Pennycott, Dario Wyss, Heike Vallery, Verena Klamroth-Marganska, and Robert Riener. Towards more effective robotic gait training for stroke rehabilitation: a review. *Journal of NeuroEngineering and Rehabilitation*, 9(1):65, Jan 2012.

[46] Jooeun Ahn and Neville Hogan. Walking Is Not Like Reaching: Evidence from Periodic Mechanical Perturbations. *PLoS ONE*, 7(3):e31767, Mar 2012.

[47] Alan T Asbeck, Stefano M.M. De Rossi, Ignacio Galiana, Ye Ding, and Conor J Walsh. Stronger, Smarter, Softer: Next-Generation Wearable Robots. *IEEE Robotics & Automation Magazine*, 21(4):22–33, Dec 2014.

[48] Steven H. Collins, M. Bruce Wiggin, and Gregory S. Sawicki. Reducing the energy cost of human walking using an unpowered exoskeleton. *Nature*, 522(7555):212–215, Apr 2015.

Appendix A. Proof of the Saddle Principal Direction Equations

The Saddle Surface principal directions' equations can be calculated with euclidean geometry by expressing the CoM height as function of its distances from the two extrapolated CoPs in 3D Cartesian coordinates as

$$\begin{cases} h_{RCoM} = \sqrt{(h_{RF}^2 - (x - x_{CoPr})^2 - (y - y_{CoPr})^2} \\ \\ h_{LCoM} = \sqrt{h_{LF}^2 - (x - x_{CoPl})^2 - (y - y_{CoPl})^2} \end{cases} \tag{A.1}$$

If we assume that both feet are in contact with the ground (double support) then the following relationship is valid.

$$\begin{aligned} & h_{RF}^2 - (x - x_{CoPr})^2 - (y - y_{CoPr})^2 = \\ & = h_{LF}^2 - (x - x_{CoPl})^2 - (y - y_{CoPl})^2 \end{aligned} \tag{A.2}$$

Which allows to derive the equation for one of the principal direction of the saddle surface, as follows:

$$\begin{aligned} y &= \tfrac{2(x_{CoPr} - x_{CoPl})}{2(y_{CoPl} - y_{CoPr})} x + \tfrac{h_{RF}^2 - h_{LF}^2 + x_{CoPl}^2 - x_{CoPr}^2 + y_{CoPl}^2 - y_{CoPr}^2}{2(y_{CoPl} - y_{CoPr})} = \\ &= \tfrac{d_{AP}}{d_{ML}} x + \tfrac{h_{RF}^2 - h_{LF}^2 + x_{CoPl}^2 - x_{CoPr}^2 + y_{CoPl}^2 - y_{CoPr}^2}{2 d_{ML}} = \\ &= m_\perp x + C_\perp \end{aligned} \tag{A.3}$$

where (x, y) are the TS coordinates, d_{AP} is the distance of the feet in the anteroposterior direction, d_{ML} is the distance between the feet in the mediolateral direction, $m_\perp$ is the slope and $C_\perp$ is the intersection with the TS frame used for both the CoM and the extrapolated CoPs positions. Furthermore, the slope of the line in equation (A.1) ($m_\perp$) describes the saddle principal that we have aligned with x_{Saddle}. Instead, y_{Saddle} is

defined by the direction of the segment connecting the fulcra of the two pendula (i.e., extrapolated CoPs).

$$\begin{aligned} y &= \frac{d_{ML}}{d_{AP}}(x - x_{CoPr}) + y_{CoPr} = \\ &= m_{//}x + \frac{x_{CoPl}y_{CoPr} - x_{CoPr}y_{CoPl}}{x_{CoPl} - x_{CoPr}} = m_{//}x + C_{//} \end{aligned} \tag{A.4}$$

where the intersection between Equations (A.3) and (A.4) is the position in TS coordinates of the saddle point (x_{S0}, y_{S0}), defined as:

$$\begin{aligned} x_{S0} &= \frac{m_{S_\perp}(C_{S_{//}} - C_{S_\perp})}{m_{S_\perp}^2 + 1} \\ y_{S0} &= \frac{(C_{S_{//}} - C_{S_\perp})}{m_{S_\perp}^2 + 1} + C_{S_{//}} \end{aligned} \tag{A.5}$$

Appendix B. Markers' Set

The CoM position and orientation on the transverse plane were calculated relying on the four pelvic markers, which are placed two on the Anterior Superior Iliac Spine and two on the Posterior Superior Iliac Spine. The position is derived as follow:

$$\begin{cases} x_{CoM}(k) = \frac{x_{LASIS}(k) + x_{RASIS}(k) + x_{LPSIS}(k) + x_{RPSIS}(k)}{4} \\ y_{CoM}(k) = \frac{y_{LASIS}(k) + y_{RASIS}(k) + y_{LPSIS}(k) + y_{RPSIS}(k)}{4} \end{cases} \tag{B.1}$$

The following equation allows to compute the extrapolated CoPs using the Heel marker, the 1^{st} and 5^{th} Metatarsal Bones.

$$\begin{cases} x_{CoP}(k) = \frac{2x_{Heel}(k) + x_{MT1}(k) + x_{MT5}(k)}{4} \\ y_{CoP}(k) = \frac{2y_{Heel}(k) + y_{MT1}(k) + y_{MT5}(k)}{4} \\ z_{CoP}(k) = \frac{2z_{Heel}(k) + z_{MT1}(k) + z_{MT5}(k)}{4} - z_{CoPg} \\ Where: \\ z_{CoP_{ground}} = \frac{2z_{Heel_{ground}} + z_{MT1_{ground}} + z_{MT5_{ground}}}{4} \end{cases} \tag{B.2}$$

While the foot orientations are derived as follows.

$$\begin{cases} \Delta x_{Foot}(k) = \frac{x_{MT1}(k)+x_{MT5}(k)}{2} - x_{Heel}(k) \\ \Delta y_{Foot}(k) = \frac{y_{MT1}(k)+y_{MT5}(k)}{2} - y_{Heel}(k) \\ \theta_{Footxy} = atan2(\frac{\Delta y_{Foot}(k)}{\Delta x_{Foot}(k)}) \\ D_{xy}(k) = \sqrt{((\Delta x_{Foot}(k))^2 + (\Delta y_{Foot}(k))^2)} \\ \Delta z_{Foot}(k) = \frac{z_{MT1}(k)+z_{MT5}(k)}{2} - z_{Heel}(k) \\ \theta_z(k) = atan2(\frac{\Delta z_{Foot}(k)}{D_{xy}(k)}) \end{cases} \tag{B.3}$$